ELSEVIER

18 April 1997

Chemical Physics Letters 268 (1997) 313–320

CHEMICAL PHYSICS LETTERS

A CCSD(T) and DFT investigation of *m*-benzyne and 4-hydroxy-*m*-benzyne

Elfi Kraka [a], Dieter Cremer [a], Götz Bucher [b], Holger Wandel [b], Wolfram Sander [b]

[a] *Department of Theoretical Chemistry, University of Göteborg, Kemigården 3, S-41296 Göteborg, Sweden*
[b] *Lehrstuhl für Organische Chemie der Ruhr-Universität, D-44780 Bochum, Germany*

Received 31 January 1997; in final form 27 February 1997

Abstract

4-Hydroxy-*m*-benzyne (**2a**), which is interesting in connection with research on enediyne antitumor drugs, has been identified by comparing the measured infrared spectrum with vibrational spectra calculated at the CCSD(T)/6-31G(d,p) and B3LYP/6-31G(d,p) levels of theory. Although the vibrational spectra of phenol and **2a** are similar, there are several infrared bands that make an identification of **2a** in the matrix at low temperatures possible. Molecule **2a** possesses the structure of a σ-biradical. Its isomer bicyclo[3.1.0]hexatriene is not stable, which is parallel to the result obtained for the parent molecule *m*-benzyne (**1**). The biradical character of **2a** is somewhat lower than that of **1**.

1. Introduction

Benzynes (dehydrobenzenes) are being investigated by many research groups since they are considered important intermediates in the DNA-cleaving reaction of enediyne antibiotics [1,2]. In the naturally occurring enediyne cytostatica, *p*-benzynes are the intermediates that abstract hydrogen from the sugar phosphate backbone of DNA and, by this, lead to a double-stranded DNA cleavage and to cell death. Clearly, the natural enediyne cytostatica are optimized to fulfil under certain conditions a specific biological task and not necessarily that of a useful anticancer drug. Therefore, ongoing research focuses on replacing the natural 'warhead' [1] of the enediyne cytostatica, namely *p*-benzyne, by a synthetic one, which is more suitable for an anticancer drug [2]. After the first successful matrix isolation and spectroscopic characterization of *m*-benzyne (**1**) by Marquardt et al. [3] substituted **1** (**2**) is the strongest candidates to fulfil the function of a 'biological warhead' for the enediyne cytostatica. The biradical **1** is more stable than *p*-benzyne [4] and, accordingly, can be better handled in experiments. Because of this, **1** and substituted **1** are of interest to synthetic chemists, spectroscopists, structural chemists, and theoreticians.

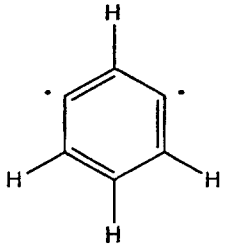

1

PII S0009-2614(97)00233-9

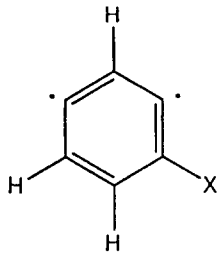

2 **2a:** X = OH

For a long time it was not clear whether *m*-benzynes exist as aromatic σ-biradicals (e.g., **1** and **2**) or highly strained bicyclic compounds (**3** and **4**).

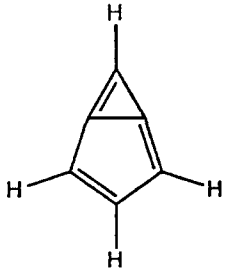

3

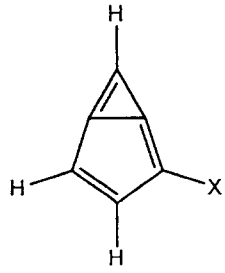

4 **4a:** X = OH

In the literature evidence, for both structures can be found: Washburn and co-workers [6] investigated the dehydrobromination of dibromobicyclo[3.1.0]hexene and obtained evidence for the existence of **3** while Billups and co-workers [7] obtained evidence for a σ-biradical structure although the synthesis of a bicyclo[3.1.0]hexatriene **4** had been attempted. The question whether structure **1** (**2**) or **3** (**4**) represents the equilibrium structure of *m*-benzynes was first answered by Sander and co-workers, who managed to trap **1** and hydroxy-substituted **1** (**4a**) in the matrix at low temperature and to measure the infrared spectrum of both compounds [3,5]. A CCSD(T) (coupled cluster calculations with all single (S) and double (D) excitations and a perturbative treatment of all triple (T) excitations [8]) investigation of the vibrational spectrum of **1** made it possible to identify all infrared bands of **1** in the experimental spectrum and, by this, provided clear evidence that (a) **1** had been trapped in the matrix and (b) the molecule exists as a biradical rather than the highly strained bicyclus **3**. Also it was found that the biradical character of **1** is just 20% since the single electrons can delocalize to some extent by through-bond interactions involving the σ^*-orbitals of vicinal CC bonds of the benzene ring.

In the case of the hydroxy derivative **2a**, an attempted identification with the help of a GVB simulation of the measured IR spectrum was less successful since a correlation of measured and calculated infrared bands was not possible [5]. In this work, we present a CCSD(T) investigation of **2a** and its properties. In particular, we investigate its vibrational spectrum and provide a detailed analysis of all vibrational modes of **2a**. We provide evidence that the infrared spectrum measured by Sander and co-workers [5] is indeed that of **2a**, and that **2a** also exists as a σ-biradical and not as bicyclus **4a**. In addition, we show that the results of the expensive CCSD(T) investigation can be reproduced with the much cheaper density functional theory (DFT). This latter observation opens a way for more extended investigations of larger σ-biradicals which are of direct biochemical interest.

2. Computational methods

CCSD(T) [8] geometry optimizations using analytical energy gradients have been carried out for **2a** using the standard 6-31G(d,p) basis set [9]. Vibrational frequencies and infrared intensities of **2a** have been obtained by combining analytical and numerical derivative techniques. Results have been compared with previous CCSD(T)/6-31G(d,p) calcula-

tions carried out for **1** utilizing the same techniques [3]. Calculations have been repeated for at the DFT level for σ-biradicals **1** and **2a** and extended to **3** and **4a** using Becke's three parameter functional B3LYP [10,11] for which analytical first and second derivatives are available.

Calculated vibrational modes were investigated using the adiabatic mode analysis of Konkoli and Cremer [12]. This approach is based on a decomposition of normal modes in terms of adiabatically relaxed internal parameter modes that are not contaminated by any other mode of the molecule. As has been shown previously the adiabatic mode analysis is superior to the potential energy distribution (PED) analysis and provides reliable internal frequencies that can directly be assigned to the internal parameters of a molecule [13]. Both internal coordinates and symmetry coordinates have been used to determine the adiabatic modes of **1** and **2a**. For all molecules considered, zero point energy (ZPE) and thermal corrections have been determined to evaluate reaction enthalpies at 298 K. Calculations were carried out with the COLOGNE96 [14], ACES [15], and GAUSSIAN94 ab initio packages [16].

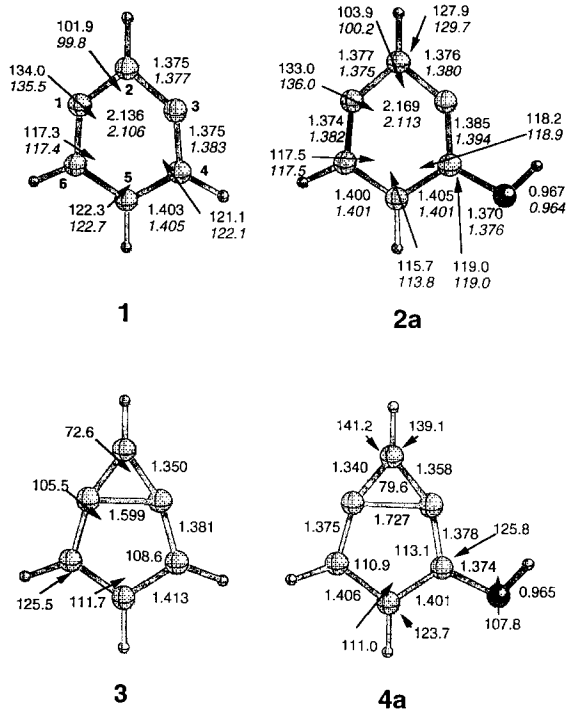

Fig. 1. CCSD(T)/6-31G(d,p) (in italics) and B3LYP/6-31G(d,p) geometries of *m*-benzynes **1** and **2a**. B3LYP/6-31G(d,p) geometries of the corresponding bicyclic molecules **3** and **4a** are also given. Distances in Å, angles in deg.

3. Results and discussion

The calculated geometries of **1** and **2a** (Fig. 1) are similar, and independent of the method used. Both CCSD(T) and B3LYP geometries reveal the typical distortion of the benzene hexagon when benzene is converted into **1** (symmetry lowering from D_{6h} to C_{2v}). The distance C1 · · · C3 is reduced from about 2.4 to 2.1 Å while the C6C1C2 angle widens from 120 to about 135°. These distortions increase ring strain, but should also lead to stabilization of the molecule. First, stabilizing through-space interactions between centers C1 and C3 increase because of the shorter distance and rehybridization of a sp^2 orbital, previously used for CH bonding, to a hybrid orbital with more p-character that extends more toward the interior of the ring and overlaps more effectively with its counterpart at C3. Secondly, rehybridization improves the π-type overlap with the σ^* orbitals of bonds C4C5 and C6C5 and in this way increases stabilizing through-bond interactions. Finally, CH bond eclipsing strain in the back part of the molecule (C4, C5, C6) is somewhat relieved (HCC angles widen to 122°). The calculated geometries of both **1** and **2a** reflect these effects. For example, the slight shortening of bonds C1C6 and C3C4 is connected to the slight lengthening of bonds C5C6 and C4C5 where both effects are due to through-bond interactions between orbitals at C1 and C3. The shortening of bonds C1C2 and C2C3 reflects the fact that steric repulsion between the CH bonds is not present in this part of the molecule.

The effect of an OH substituent on the electronic structure of **1** can best be analyzed when considering first its energetical influence with the help of appropriate formal reactions:

$$\text{benzene} + CH_3OH \rightarrow \text{phenol} + CH_4\,, \quad (1)$$

$$\mathbf{1} + CH_3OH \rightarrow \mathbf{2a} + CH_4\,, \quad (2)$$

$$\mathbf{1} + \text{phenol} \rightarrow \mathbf{2a} + \text{benzene}\,, \quad (3)$$

$$\mathbf{2a} + H_2 \rightarrow \text{phenol}\,, \quad (4)$$

$$\mathbf{2a} + CH_3CH_3 \rightarrow \text{phenol} + CH_2{=}CH_2\,. \quad (5)$$

The reaction energies of (1)–(5) haven been calculated at the B3LYP/6-31G(d,p) level of theory, corrected by the differences in the corresponding ZPE, and checked by comparing with CCSD(T) reaction energies. Reactions (1) and (2) provide an insight into the stabilization of benzene or **1** by an OH group, which is −14.4 kcal/mol in the first and −10.8 kcal/mol in the second case suggesting that OH substitution of **1** is 3.4 kcal/mol less stabilizing than in the case of benzene. On the other hand, one can derive from the OH rotational potential of **2a** that **2a** is at the same time significantly stabilized due to reduced CH bond eclipsing. The conformation with the OH rotated by 180° (rotational barrier at 90°: 4.6 kcal/mol; phenol: 4.1 kcal/mol at B3LYP/6-31G(d,p)) is 3.4 kcal/mol less stable than the equilibrium form, which suggests that deformation of the benzene hexagon and reduced π-delocalization correspond to at least 6.8 kcal/mol and that this value is lowered to 3.4 kcal/mol (calculated from reactions 1 and 2) due to more favourable steric interactions. π-Conjugation of the OH group with the benzene ring should lengthen bonds C3C4, C4C5, C1C2, and C1C6 while bonds C2C3 and C5C6 should be shortened, which is confirmed by the calculated geometry of phenol. In **2a**, there is a superposition of the π-conjugation and the through-bond effect, which leads to a reduction of the π-stabilisation effect (see **5**).

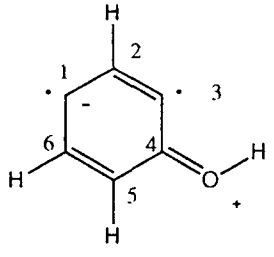

5

Reactions (3), (4), and (5) can be used to calculate the (unknown) heat of formation of **2a**. For this purpose, calculated reaction enthalpies are combined with known reaction enthalpies of benzene (19.8), phenol (−23.0), *m*-benzyne (122.8 [4]), ethane (−20.2) and ethene (12.4 kcal/mol) [17]. Using reaction (3), ΔH_f^0 of **2a** is calculated to be 83.4 kcal/mol. With reactions (4) and (5), ΔH_f^0(**2a**) = 86.0 and 85.5 kcal/mol are obtained. In view of the relatively large uncertainty of ΔH_f^0 for **1** [4], we suggest a value of 85 ± 1 kcal/mol.

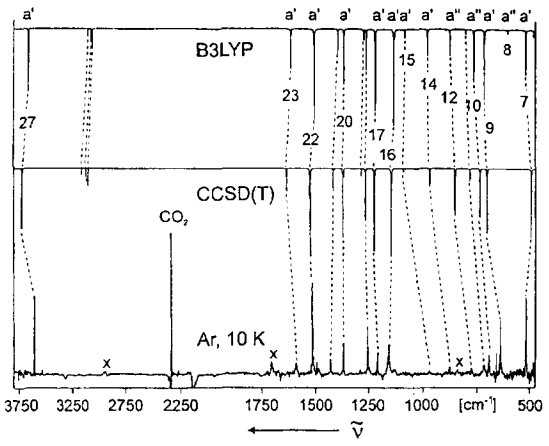

Fig. 2. B3LYP/6-31G(d,p), CCSD(T)/6-31G(d,p), and experimental infrared spectrum of 4-hydroxy-*m*-benzyne **2a**. A scaling factor of 0.960 has been used. The numbering of frequencies corresponds to the numbering used in Table 1.

Bicyclic molecules **3** and **4a** are both minima at the B3LYP/6-31G(d,p) level of theory, being more stable by 2.6 and 1.2 kcal/mol, respectively, than the corresponding biradicals. However, the minima vanish at the CCSD(T) level. Utilizing B3LYP geometries, CCSD(T) predicts **3** and **4a** 3.0 and 3.5 kcal/mol higher in energy than the σ-biradicals **1** and **2a**.

In Fig. 2, B3LYP/6-31G(d,p), CCSD(T)/6-31G(d,p) and experimental infrared spectrum of hydroxy-benzyne **2a** are compared (data are listed in Table 1). Compound **2a** was generated by irradiation of the quinone diazide **5** in a matrix with visible light (argon 10 K, $\lambda > 470$ nm). In the first step of the reaction, the intermediate **6** is formed, which could be verified by narrow-band irradiation ($\lambda > 432 \pm 10$ nm, 90 min) of **5** and subsequent investigation by IR and UV/VIS spectroscopy.

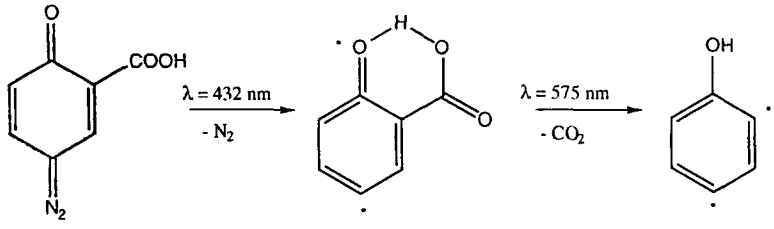

5 6 2a

Irradiation of the long-wavelength absorption band of **6** ($\lambda > 575 \pm 10$ nm, 20 min) led to rapid decarboxylation (intense infrared absorption of CO_2 at 2347 cm^{-1}, see Fig. 2) and the formation of **2a**. *m*-Benzyne **2a** is stable to irradiation with $\lambda > 570$ nm, however short-wavelength light ($\lambda > 420$ nm) converts it into a ketene. To verify that the measured infrared bands shown in Fig. 2 belong to one and the same molecule, the infrared spectrum was also recorded after ketene formation.

All measured infrared bands can be assigned with the help of the calculated spectra where one has to consider that in the experiment the concentration of **2a** is rather small and, accordingly, the intensity of its infrared bands is also rather small compared to the intensity of the CO_2 band. The agreement between measured and calculated frequencies is reasonable in the region between 1200 and 1600 cm^{-1} but deteriorates in the region below 1000 cm^{-1} (Fig. 2). In the latter region, the frequencies of ring deformation and H out-of-plane modes are found. Any ring deformation involving the radical centers is more difficult to describe by a given method and basis set than those vibrational modes that do not involve the radical centers. Although both CCSD(T) and B3LYP should cover the most important correlation effects, we note that due to limitations in particular in the CCSD(T) calculation the VDZP basis set used is still modest for the problem of describing **2a**. A cc-TZ2P basis set should lead to better results as we could show in the case of smaller molecules. Some of the deviations between measured and calculated frequencies may be reduced by using group scaling factors. For example, it is obvious that for the OH stretching frequency a scaling factor of 0.93 rather than an average scaling factor of 0.96 used in this work is more appropriate. However, we have refrained from improving the agreement between measured and calculated frequencies by utilizing group scaling factors since for derivation of the latter the available information is not sufficient.

The infrared spectrum of **2a** resembles that of phenol. Characteristic for the latter are the OH stretching band at 3623 (B3LYP: 3812, scaled with 0.96: 3660) cm^{-1}, the COH bending band at 1180 (1202, 1154), and the OH torsion band at 241 (351, 337) cm^{-1} (see Fig. 3). These bands appear in the spectrum of **2a** almost at the same positions (compare Fig. 2 with Fig. 3) and, therefore, do not provide a possibility to distinguish between phenol and **2a**. However, a distinction is possible in the range 1700 to 1400 cm^{-1} where CC stretch and CCH bending modes lead to the band pattern small–large–small–large in the case of **2a** while phenol has in this region three infrared bands (pattern: large–large–large) where the first band actually consists of two lines. Similar differences are in the region between 1000 and 500 cm^{-1} where in the case of phenol a triplet of infrared bands (pattern: smaller–larger–smaller) at 700 cm^{-1} is dominant arising from H out-of-plane bending, CCC ring bending, and chair-type ring torsion motions. In the case of **2a**, there are two larger bands at 500 and at 650 cm^{-1} and three smaller bands between 700 and 1000 cm^{-1}.

Fig. 4, gives a correlation of the calculated vibrational spectra of phenol, hydroxy-*m*-benzyne **2a**, and *m*-benzyne **1**, which is based on the adiabatic mode analysis of Konkoli and Cremer [12]. This correlation reveals that the central line of the triplet at 700 cm^{-1} and two smaller peaks directly after the COH bending band of phenol involve motions of the H atoms absent in **2a** and, therefore, cannot appear in the infrared spectrum of **2a**. The correlation pattern in Fig. 4 helps to assign all measured infrared bands and to understand the differences in the electronic structures of **1**, **2a**, and phenol. The information

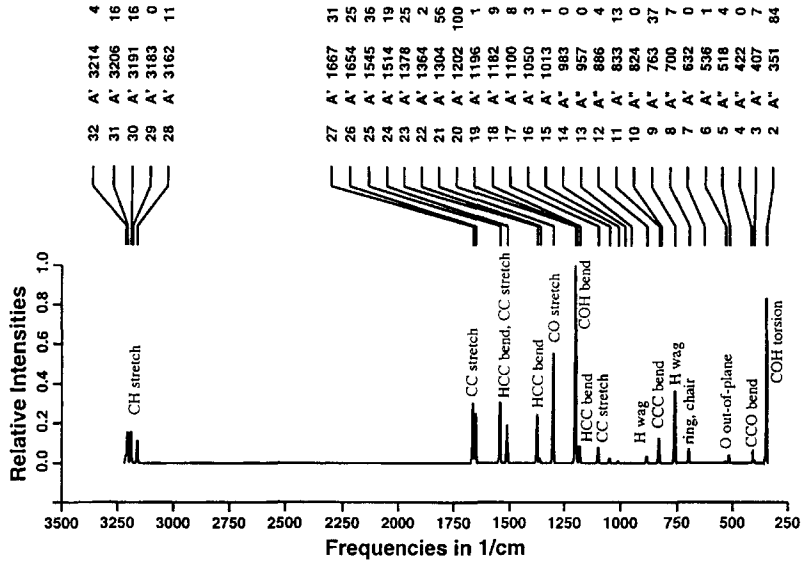

Fig. 3. B3LYP/6-31G(d,p) infrared spectrum of phenol. The vibrational modes have been characterized with the help of the adiabatic mode analysis.

obtained in Fig. 4 is complemented by a graphical representation of the adiabatic mode frequencies summarized in Fig. 5. Adiabatic frequencies of stretching modes are related to bond lengths (shorter bond lengths lead to larger frequencies), but reflect also some environmental effects as, e.g., eclipsing effects of bonds attached to the bond in question. Thus, the adiabatic stretching frequency of C1C2 is considerably smaller in **1** (last entry: 1218 cm^{-1}, Fig. 5) than in phenol (first entry: 1367 cm^{-1}).

Adiabatic bending and torsional frequencies reflect the stiffness of the benzene ring, which is

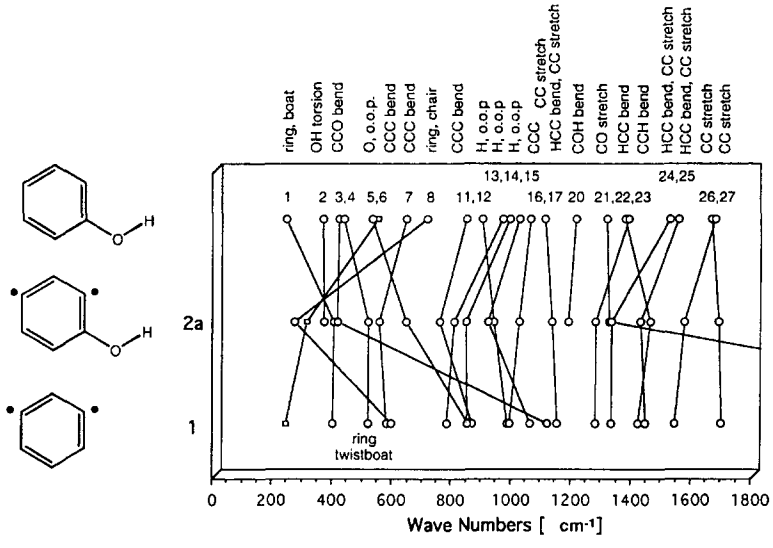

Fig. 4. Correlation of the B3LYP/6-31G(d,p) vibrational frequencies of phenol, 4-hydroxy-*m*-benzyne **2a**, and *m*-benzyne **1** in the range 0–1800 cm^{-1}. For phenol, the vibrational modes are characterized in short form (compare with Fig. 3). Modes 9, 10, 18, and 19 of phenol are missing since they correspond to the H out-of-plane and HCC bending motions of the two H atoms absent in benzynes.

considerably reduced by the absence of the CH bonds in positions C1 and C3. This is parallel to the decrease in the frequency of the chair-type out-of-plane torsion of the ring and CCC bending (entry no. 6).

In conclusion, hydroxy-*m*-benzyne **2a** has positively been identified via its infrared spectrum. CCSD(T) calculations suggest that **2a** possesses the structure of a σ-biradical which has just 15% biradical character using **1** (biradical character: 20% [4]) as an appropriate reference. The hydroxy-substituted bicyclus **4a** would have a ring stretching mode with weak intensity above 1700 cm^{-1} by which it can be identified. However, CCSD(T) calculations show that the bicyclic isomer **4a** is not stable. Another important result of this work is that *m*-arynes can be rather well described at the CCSD(T) level of theory, which is not surprising, but also at the B3LYP level, which reduces calculational cost considerably in this case and provides a promising basis for further investigations on *m*-arynes.

Table 1
Calculated and measured vibrational frequencies ω and infrared intensities *I* of 4-hydroxy-*m*-benzyne [a]

No.	Symm.	CCSD(T)		B3LYP		Exp.	
		ω	*I*	ω	*I*	ω	*I*
1	a″	251	0.0	259	0.0		
2	a″	320	133.3	358	126.7		
3	a′	332	7.7	300	20.8		
4	a″	356	5.3	389	4.0		
5	a′	436	1.3	420	2.0		
6	a″	445	2.4	504	4.2		
7	a′	516	65.4	541	32.4	519	s
8	a″	530	0.3	632	2.4		
9	a′	735	58.0	745	63.2	641	s
10	a″	769	37.4	796	36.1	695	m
11	a″	817	7.7	835	2.6	718	w
12	a″	882	0.7	929	0.4		
13	a′	889	35.6	910	16.6	774	w
14	a′	1008	11.4	1015	16.9	877	w
15	a′	1134	2.5	1122	4.8	972	w
16	a′	1195	116.9	1178	134.3	1157	m
17	a′	1275	97.7	1266	84.5	1209	m
18	a′	1317	42.0	1310	28.6	1255	m
19	a′	1336	4.8	1320	6.1		
20	a′	1426	64.9	1418	42.5	1368	m
21	a′	1475	15.4	1448	15.1	1429	w
22	a′	1589	118.5	1564	108.2	1516	s
23	a′	1703	15.4	1678	27.5	1592	w
24	a′	3232	11.2	3180	10.4		
25	a′	3254	8.3	3200	6.1		
26	a′	3295	3.9	3228	2.7		
27	a′	3880	51.7	3817	51.4	3612.0	m

[a] Frequencies ω in cm^{-1}, intensities *I* in km/mol. In the case of the experimental data, relative intensities are given. The experimental spectrum was measured only above 500 cm^{-1}.

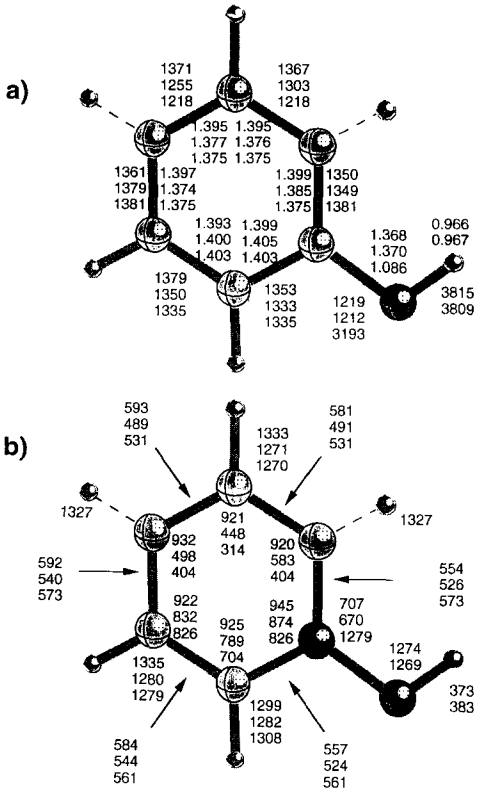

Fig. 5. Adiabatic Frequencies of phenol (first entry), 4-hydroxy-*m*-benzyne **2a** (second), and *m*-benzyne **1** (third) calculated at the B3LYP/6-31G(d,p) level of theory. The position of the H atoms missing in **1** and **2a** is indicated for phenol. (a) Adiabatic stretching frequencies and calculated bond lengths for CC, CO, and OH bonds. (b) Adiabatic CH stretching, CCC and COH bending, and CCCC (indicated by arrows; CCOH without arrow) torsional frequencies. All frequency values in cm^{-1}. (B3LYP/6-31G(d,p) calculations.)

Acknowledgements

This work was supported at the University of Göteborg by the Swedish Natural Science Research Council (NFR) and at the Universität Bochum by the

Deutsche Forschungsgemeinschaft and the Fonds der Chemischen Industrie. Calculations were done on a CRAY YMP/464 and CRAY C90 of the Nationellt Superdatorcentrum (NSC), Linköping, Sweden. This work required a large amount of computer time and would not have been possible without the support of the NSC. EC and DC thank the NSC for a generous allotment of computer time.

References

[1] K.C. Nicolaou, W.M. Dai, Angew. Chem. Int. Ed. Engl. 30 (1991) 1387.
[2] P. Chen, Angew. Chem. 108 (1996) 1584.
[3] R. Marquardt, W. Sander, E. Kraka, Angew. Chem. Int. Ed. Engl. 35 (1996) 746.
[4] E. Kraka, D. Cremer, Chem. Phys. Lett. 216 (1993) 333. E. Kraka, D. Cremer, J. Am. Chem. Soc. 116 (1994) 4929.
[5] G. Bucher, W. Sander, E. Kraka, D. Cremer, Angew. Chem. Int. Ed Engl. 31 (1992) 1230.
[6] W.N. Washburn, J. Am. Chem. Soc. 97 (1975) 1615.
[7] W.E. Billups, J.D. Buynak, D. Butler, J. Org. Chem. 44 (1979) 4218.
[8] K. Raghavachari, G.W. Trucks, J.A. Pople, M. Head-Gordon, Chem. Phys. Lett. 157 (1989) 479.
[9] P.C. Hariharan, J.A. Pople, Chem. Phys. Lett. 66 (1972) 217.
[10] A.D. Becke, J. Chem. Phys. 98 (1993) 5648.
[11] P.J. Stephens, F.J. Devlin, C.F. Chablowski, M.J. Frisch, J. Phys. Chem. 98 (1994) 11623.
[12] Z. Konkoli, D. Cremer, to be published.
[13] Z. Konkoli, A. Larsson, D. Cremer, to be published.
[14] E. Kraka, J. Gauss, F. Reichel, Zhi He, L. Olsson, Z. Konkoli, D. Cremer, COLOGNE 96, Göteborg, 1996.
[15] J.F. Stanton, J. Gauss, J.D. Watts, W.J. Lauderdale, R.J. Bartlett, ACES II, Quantum Theory Project, University of Florida, 1992.
[16] M.J. Frisch, M. Head-Gordon, G.W. Trucks, J.B. Foresman, H.B. Schlegel, K. Raghavachari, M.A. Robb, J.S. Binkley, C Gonzalez, D.J. DeFrees, D.J. Fox, R.A. Whiteside, R. Seeger, C.F. Melius, J. Baker, R.L. Martin, L.R. Kahn, J.J.P. Stewart, S. Topiol, J.A. Pople, Gaussian 94, Gaussian, Pittsburgh, PA, 1994.
[17] J.D. Cox, G. Pilcher, Thermochemistry of Organic and Organometallic Compounds, Academic Press, New York, 1970.